

## Surface structure of cesium adsorption on the Si(001) $2 \times 1$ surface

H. Hamamatsu

*Department of Chemistry, Graduate School of Science, The University of Tokyo, Hongo, Bunkyo-ku, Tokyo 113, Japan*

H. W. Yeom

*Research Center for Spectrochemistry, Faculty of Science, The University of Tokyo, Hongo, Bunkyo-ku, Tokyo 113, Japan*

T. Yokoyama, T. Kayama, and T. Ohta

*Department of Chemistry, Graduate School of Science, The University of Tokyo, Hongo, Bunkyo-ku, Tokyo 113, Japan*

(Received 30 September 1997; revised manuscript received 5 December 1997)

The detailed surface structure of Cs adsorption on the Si(001)  $2 \times 1$  surface was investigated by means of tensor low-energy electron diffraction analysis. Various adsorption sites were considered including the recently proposed possibility of asymmetric dimer reconstruction of the Si top layer. We confirm the structure model with double-layer adsorbates and symmetric Si dimers underneath for the saturation coverage Cs adsorption. The major structural parameters within this structure are discussed in terms of the covalent bonding between the adsorbates and Si surface atoms. [S0163-1829(98)06016-0]

### I. INTRODUCTION

Adsorption of alkali metals (AM's) on semiconductor surfaces has been studied for decades as a prototype of semiconductor-metal interfaces.<sup>1</sup> A model system for such studies has been AM adsorption on the Si(001)  $2 \times 1$  surface. As for this extensively studied surface, a structure model with one-dimensional AM chains, where AM atoms adsorb on the pedestal site [*HH*, denoted as in Fig. 1(a)], was proposed first<sup>2</sup> for AM saturated surfaces at room temperature and was supported by an anisotropic plasmon dispersion observed by electron energy-loss spectroscopy.<sup>3</sup>

Later the semiconducting surface band structure<sup>4</sup> was observed for the K saturated surface in contradiction to the one-dimensional AM chain model. The so-called double-layer model with a monolayer (ML) of AM adsorbates was proposed by Abukawa and Kono to explain x-ray photoelectron diffraction patterns<sup>5,6</sup> and the semiconducting surface electronic structures. This model was subsequently supported by various experimental<sup>7-10</sup> and theoretical<sup>11,12</sup> works. However, although there are some objections regarding this model even in recent literature,<sup>13</sup> very recent high-resolution photoemission studies<sup>14,15</sup> confirmed the validity of this model again. Furthermore the recent high-resolution photoemission study<sup>15</sup> proposed a possibility of Si dimer buckling beneath the Cs adsorbates unlike the other AM adsorbates.

At present, the debates on the saturation-coverage surface structures and electronic structures are still underway.<sup>16</sup> Other than this long-standing and ongoing debates, there are also relevant controversies regarding basic issues such as the nature of bonding between the alkali metals and Si surfaces,<sup>17</sup> and metallization at the saturation coverage.<sup>15</sup>

In this paper, we report a low-energy electron diffraction (LEED) intensity versus voltage (*I-V*) analysis of the saturated Cs adsorption on the Si(001)  $2 \times 1$  surface. Several structure models with Cs coverages of 0.5 and 1.0 ML with different adsorption sites were tested. A similar structure

analysis was reported for K and Cs adsorption previously,<sup>10</sup> but the present study performed more extensive investigation in both experiments and calculations. In addition, the newly proposed possibility of Si asymmetric dimer buckling<sup>15</sup> was also considered. The present results confirm the double-layer model with the symmetric Si dimer for the room-temperature Cs saturated surface. The detailed structural parameters determined are discussed to understand the mechanism of the Si surface reconstruction for Cs adsorption.

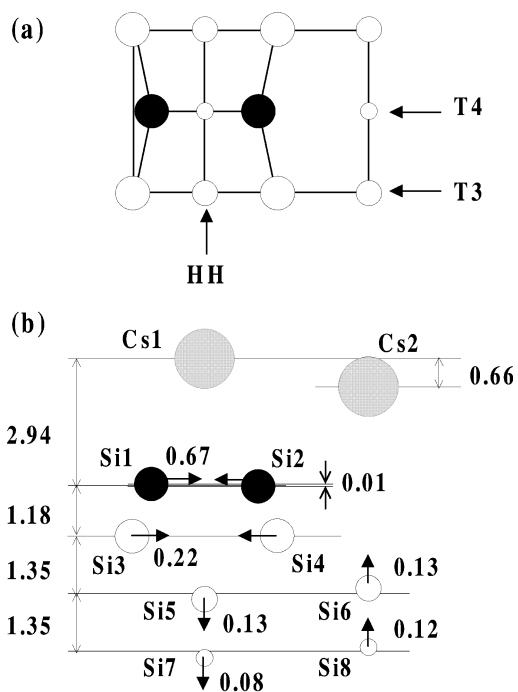


FIG. 1. Schematic drawing of (a) the adsorption sites considered for alkali metals on the Si(001)  $2 \times 1$  surface and (b) the optimized structure for the *HH+T3* model. Horizontal and vertical displacements from the ideal bulk positions are given in the Å unit.

## II. EXPERIMENTS AND ANALYSES

LEED experiments were performed in an ultrahigh vacuum (UHV) chamber pumped by a turbo molecular pump and a Ti sublimation pump (typically down to  $9 \times 10^{-9}$  Pa). It was equipped with a commercial four-grid LEED optics (OMICRON), an x-ray tube and a hemispherical electron energy analyzer. A Si(001) wafer was chemically treated by the standard Shiraki method<sup>18</sup> before mounting into the chamber. It was then cleaned by careful stepwise annealing up to 1250 K in UHV, and finally showed sharp  $(2 \times 1)$  LEED patterns. Cs was evaporated onto the Si(001)  $2 \times 1$  surface at room temperature from a well outgassed getter source (SAES Getters). The pressure never exceeded  $4 \times 10^{-8}$  Pa during the evaporation. The coverage of Cs was monitored by the change of the work function measured by the secondary electron cutoff in x-ray photoelectron spectra. A sharp  $(2 \times 1)$  LEED pattern was observed for the room-temperature saturated surface at the beginning of the plateau of the work-function change, which is consistent with the previous work.<sup>15</sup>

LEED  $I$ - $V$  curves were measured at room temperature with a cooled charge-coupled device camera controlled by a computer. The intensities of LEED spots were measured with normal incidence of the primary electron beam, which was acquired by a precise alignment mechanism of the sample manipulator.  $I$ - $V$  curves of the equivalent symmetric beams were almost identical and hence were averaged. The data set consists of five integral-order and two fractional-order beams in the energy range of 50–250 eV, amounting to the total-energy range of 958 eV.

LEED  $I$ - $V$  analyses were carried out by a well-established tensor LEED scheme using the SATLEED package by Barbieri and Van Hove.<sup>19</sup> For dynamical LEED calculations, up to seven partial wave phase shifts were used. Within the structure models, Si atoms down to the fourth Si layer were displaced in the vertical direction independently. Grid searches were performed on the horizontal displacements of the Si dimer structure from the ideal position as shown in Fig. 1(b). The real part of the inner potential and the thermal vibration amplitude were also optimized. The imaginary part of the inner potential was fixed to be  $-5.0$  eV. The quantitative agreements between theoretical and experimental  $I$ - $V$  curves were verified by the Pendry reliability factor  $R_p$ .<sup>20</sup> Compared to the previous LEED study for this surface,<sup>10</sup> a much wider energy range was covered for the total experimental data and more phase shifts and more structure parameters were taken into account in calculations for the reliable structure determination.

## III. RESULTS AND DISCUSSION

Experimental LEED  $I$ - $V$  curves are shown in Fig. 2. Although the experimental  $I$ - $V$  curves themselves were not identical to the previously reported ones,<sup>10</sup> especially for the  $(1\ 0)$  beam, their reproducibility was checked very carefully. These discrepancies might be due to the sample preparation or possible difference in data taking system. Tensor LEED analyses were performed for different structure models with coverages of 1.0 and 0.5 ML. Figure 1(a) shows possible Cs adsorption sites discussed in the literature<sup>11</sup> for the 0.5 ML

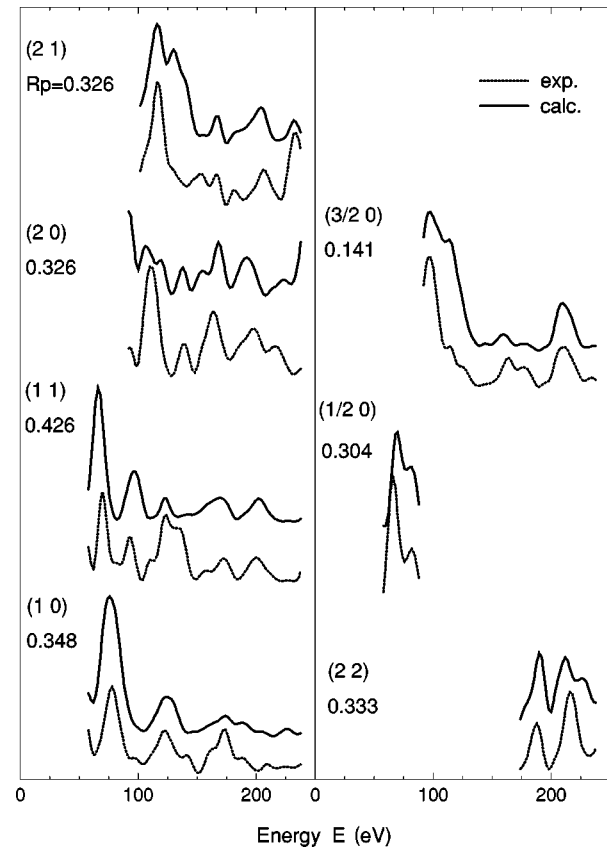


FIG. 2. Comparison of the best-fit LEED  $I$ - $V$  curves (solid lines) for the  $HH+T3$  model with experimental ones (dashed lines) for Si(001)  $2 \times 1$ -Cs. The overall Pendry  $R$  factor ( $R_p$ ) is 0.326. The  $R$  factor for each curve is also given.

coverage; pedestal ( $HH$ ), valley-bridge ( $T3$ ), and cave ( $T4$ ) sites. Since the adsorption at the bridge site on top of a Si dimer was found to be very unstable<sup>21</sup> and the off-center valley bridge site was reported only for a very low coverage,<sup>22</sup> they were not considered in the present study. We examined the combination of  $HH$  site and  $T3$  or  $T4$  site for the models with Cs coverages of 1 ML.

The  $R_p$ 's for all the structure models considered are listed in Table I. The  $HH+T3$  site model gives the smallest  $R_p$  and we obtain  $\Delta R_p = 0.067$  as the range of uncertainty on  $R_p$  for this model using the Pendry's statistical estimation.<sup>20</sup> Since the  $R_p$ 's for all of the structure models with 0.5 ML considered (see Table I) are out of this uncertainty range, the possibility of 0.5 ML models for the saturation coverage can be excluded clearly.

The models with two different Cs sites were strongly supported by the two clearly resolved components in the Cs  $4d$  photoemission spectra<sup>15</sup> and the saturation coverage of 0.98 ML measured by the medium energy ion scattering.<sup>8</sup> Two models with a 1 ML coverage were considered and the  $HH+$

TABLE I. Pendry  $R$  factor obtained for different structure models of Si(001)  $2 \times 1$ -Cs. See text for the naming of each structure model.

$HH+T3$	$HH+T4$	$T3$	$T4$	$HH$
0.326	0.541	0.448	0.630	0.459

TABLE II. The interatomic distances (in Å) determined for the  $HH+T3$  model of  $\text{Si}(001) 2 \times 1\text{-Cs}$ .

Si-Si dimer	Si3-Si4	AM1-Si2	AM2-Si2	AM2-Si4	AM
2.50	3.40	3.72	3.94	4.06	Cs (this work)
2.28	2.40	3.70	3.70	4.13	Cs (Ref. 10)
2.54	3.57	3.36	3.47	3.36	K (Ref. 11)

$T3$  model is favored exclusively against the  $HH+T4$  model from a large difference in their  $R_p$ 's as shown in Table I. This is consistent with the previous x-ray photoelectron diffraction<sup>6</sup> and LEED (Ref. 10) studies. For the extensively studied K adsorption on  $\text{Si}(001)$ , two K desorption peaks were observed in thermal desorption spectroscopy showing two different adsorption sites.<sup>7</sup> In addition, the *ab initio* calculation<sup>11</sup> concluded that K was adsorbed not only at the  $T3$  site, but also at the hollow site along the dimer chain ( $HH$  site) at 1 ML. These findings are all consistent with the present results.

Structural parameters optimized for the  $HH+T3$  model are schematically shown in Fig. 1(b) and summarized in Table II. Due to the adsorption of Cs the Si dimer bond elongates by 0.32 Å compared to the asymmetry dimer on the clean  $\text{Si}(001) 2 \times 1$  surface,<sup>23</sup> and is also longer than the previous LEED result.<sup>10</sup> This dimer bond elongation can be naturally explained by the occupation of antibonding  $\pi^*$  bands<sup>11,24</sup> of Si dimer dangling bonds by the donation of valence electrons from Cs adsorbates. In the previous LEED study,<sup>10</sup> the interatomic distance between Si atoms in the second layer is comparable to that of the Si dimer, this implying that the dimer bonds are almost perpendicular to the back bonds ( $92^\circ$ ). On the other hand, the angle is  $101^\circ$  in the present work, which is closer to the value of ideal  $sp^3$  configuration of  $109.5^\circ$ . In Fig. 1(b), the bulk interlayer spacing of the  $\text{Si}(001)$  surface is shown below the second Si layer. The sublayer Si atoms Si5 and Si7 move downward from the bulk position, whereas Si6 and Si8 move upward from the bulk position. Such reconstruction in the third and fourth Si layers coincides qualitatively with that of the *ab initio* calculation for  $\text{Si}(001) 2 \times 1\text{-K}$  and the recent structure analysis for the clean  $\text{Si}(001) 2 \times 1$  surface.<sup>23</sup> This general trend is understood as a reconstruction to release the local strain caused by the formation of the Si dimer.

Figure 3 shows the  $R$  factor changes as functions of (a) the vertical position of each Si dimer atom and (b) the buckling displacement of the Si dimer with their center of mass fixed at the same position. It is obvious from this figure that the Si dimer forms a symmetric dimer structure in contradiction to the interpretation of the recent high-resolution photoemission spectra.<sup>15</sup> Thus the observed difference in high-resolution Si  $2p$  core-level spectra for the K and Cs saturated surfaces<sup>14,15</sup> is thought to be caused by the photoelectron diffraction effect not by the asymmetric Si dimer reconstruction. Indeed for the Cs saturated surface an anomalously large photoelectron diffraction effect was observed very recently for the surface shifted component in Si  $2p$  spectra, which could be explained by strong photoelectron scattering by Cs adsorbates within the double-layer model and the symmetric Si dimer structure.<sup>25</sup>

The vertical separation of two Cs layers was found to be 0.66 Å. It is uncertain why this value is quite different from

that reported in Ref. 6 (1.2 Å). The average bond length between Cs and Si atoms obtained (see Table II) is 3.8 Å, which is very close to the sum of the Si covalent radius (1.1 Å) and the Cs metal radius (2.66 Å). For the K adsorption on  $\text{Si}(001)$ , Ishida and Terakura<sup>26</sup> showed that the adatom region is essentially neutral and showed the importance of the Si-K bond hybridization in a polarized covalent bonding. The bond length between K and Si, reported later<sup>11</sup> (see Table II), in such polarized covalent bonding is also close to the sum (3.4 Å) of the Si covalent radius and the K metal radius (2.31 Å). From this bond length comparison, the present results would support the covalent bonding picture for the saturation coverage Cs adsorption.

#### IV. CONCLUSIONS

The detailed surface structure of the saturation coverage Cs adsorption on the  $\text{Si}(001) 2 \times 1$  surface was successfully determined by the tensor LEED  $I$ - $V$  analysis. For the room-temperature saturated phase, the double-layer model with a symmetric Si dimer yields the smallest reliability factor, which is unambiguously distinguishable from those of the other structures considered. Important structural parameters of the optimized structure, such as the Si dimer bond length and subsurface reconstructions, are understood by the electronic structures and the local strain release in the substrate. The obtained Cs-Si bond lengths seem to support the picture of polarized covalent bonding between Cs and Si at the saturation coverage.

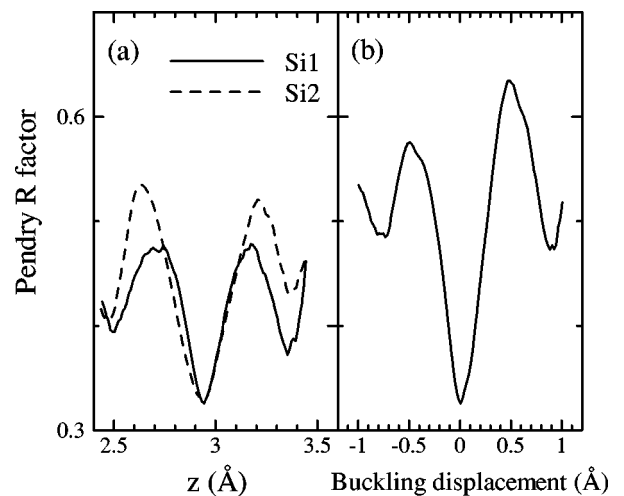


FIG. 3. Pendry  $R$  factor variations for the  $HH+T3$  model of  $\text{Si}(001) 2 \times 1\text{-Cs}$  as functions of (a) the vertical position of each Si dimer atom (Si1 and Si2, see Fig. 1) and (b) the buckling displacement (difference in the vertical positions of Si1 and Si2) of the Si dimer with their centers of mass fixed.

## ACKNOWLEDGMENTS

We acknowledge Professor M. A. Van Hove for providing the SATLEED program, and Professor Sakama for help in calculations. We are also grateful for the financial support of

the Grant-in-Aid for Scientific Research (No. 07454060). One of us (H.H.) acknowledges the financial support from the Japan Society for the Promotion of Science and the Grant-in-Aid for Scientific Research (No. 3865).

- 
- <sup>1</sup>*Metallization and Meta-Semiconductor Interfaces*, Vol. 195 of *NATO Advanced Study Institute, Series B: Physics*, edited by I. P. Batra (Plenum, New York, 1989).
- <sup>2</sup>J. D. Levine, *Surf. Sci.* **34**, 90 (1973).
- <sup>3</sup>T. Aruga, H. Tochiwara, and Y. Murata, *Phys. Rev. Lett.* **53**, 372 (1984).
- <sup>4</sup>Y. Enta, T. Kinoshita, S. Suzuki, and S. Kono, *Phys. Rev. B* **36**, 9801 (1987).
- <sup>5</sup>T. Abukawa and S. Kono, *Phys. Rev. B* **37**, 9097 (1988).
- <sup>6</sup>T. Abukawa and S. Kono, *Surf. Sci.* **214**, 141 (1989).
- <sup>7</sup>S. Tanaka, N. Takagi, N. Minami, and M. Nishijima, *Phys. Rev. B* **42**, 1868 (1990).
- <sup>8</sup>A. J. Smith, W. R. Graham, and E. W. Plummer, *Surf. Sci.* **243**, L37 (1991).
- <sup>9</sup>L. S. O. Johansson and B. Reihl, *Phys. Rev. Lett.* **67**, 2191 (1991).
- <sup>10</sup>T. Urano, S. Hongo, and T. Kanaji, *Surf. Sci.* **287/288**, 294 (1993).
- <sup>11</sup>K. Kobayashi, Y. Morikawa, K. Terakura, and S. Blügel, *Phys. Rev. B* **45**, 3469 (1992).
- <sup>12</sup>Y. Morikawa, K. Kobayashi, and K. Terakura, *Surf. Sci.* **283**, 377 (1993).
- <sup>13</sup>P. S. Mangat and P. Soukiassian, *Phys. Rev. B* **52**, 12 020 (1995).
- <sup>14</sup>Y. -C. Chao, L. S. O. Johansson, C. J. Karlsson, E. Landemark, and R. I. G. Uhrberg, *Phys. Rev. B* **52**, 2579 (1995).
- <sup>15</sup>Y. -C. Chao, L. S. O. Johansson, and R. I. G. Uhrberg, *Phys. Rev. B* **54**, 5901 (1996).
- <sup>16</sup>P. Segovia, G. R. Castro, A. Mascaraque, and E. G. Michel, *Surf. Sci.* **377-379**, 220 (1997).
- <sup>17</sup>P. Krüger and J. Pollmann, *Appl. Phys. A: Solids Surf.* **59**, 487 (1994).
- <sup>18</sup>A. Ishizaki and Y. Shiraki, *J. Electrochem. Soc.* **133**, 666 (1986).
- <sup>19</sup>A. Barbieri and M. A. Van Hove (private communication).
- <sup>20</sup>J. B. Pendry, *J. Phys. C* **13**, 937 (1980).
- <sup>21</sup>K. Kobayashi, S. Blügel, H. Ishida, and K. Terakura, *Surf. Sci.* **242**, 349 (1991).
- <sup>22</sup>T. Hashizume, Y. Hasegawa, I. Sumita, and T. Sakurai, *Surf. Sci.* **246**, 189 (1991).
- <sup>23</sup>H. Over, J. Wasserfall, W. Ranke, C. Ambiatello, R. Sawitzki, D. Wolf, and M. Moritz, *Phys. Rev. B* **55**, 4731 (1997).
- <sup>24</sup>Y. Enta, S. Suzuki, S. Kono, and T. Sakamoto, *Phys. Rev. B* **39**, 5524 (1989).
- <sup>25</sup>T. Abukawa *et al.* (unpublished).
- <sup>26</sup>H. Ishida and K. Terakura, *Phys. Rev. B* **40**, 11 519 (1989).